High glucose inhibits neural differentiation by excessive autophagy *via* peroxisome proliferator-activated receptor gamma

Ying Pan,* Di Qiu,* Shu Chen,* Xiaoxue Han, Ruiman Li

Department of Obstetrics and Gynecology, The First Affiliated Hospital of Jinan University, Jinan, Guangzhou, China
These authors contributed equally to this work

ABSTRACT

The high prevalence of prediabetes and diabetes globally has led to the widespread occurrence of severe complications, such as diabetic neuropathy, which is a result of chronic hyperglycemia. Studies have demonstrated that maternal diabetes can lead to neural tube defects by suppressing neurogenesis during neuroepithelium development. While aberrant autophagy has been associated with abnormal neuronal differentiation, the mechanism by which high glucose (HG) suppresses neural differentiation in stem cells remains unclear. Therefore, we developed a neuronal cell differentiation model of retinoic acid induced P19 cells to investigate the impact of HG on neuronal differentiation *in vitro*. Our findings indicate that HG hinders neuronal differentiation and triggers excessive apoptosis. Furthermore, HG treatment significantly reduces the expression of markers for neurons (Tuj1) and glia (GFAP), while enhancing autophagic activity mediated by peroxisome proliferator-activated receptor gamma (PPARγ). By manipulating PPARγ activity through pharmacological approaches and genetically knocking it down using shRNA, we discovered that altering PPARγ activity affects the differentiation of neural stem cells exposed to HG. Our study reveals that PPARγ acts as a downstream mediator in HG-suppressed neural stem cell differentiation and that refining autophagic activity *via* PPARγ at an appropriate level could improve neuronal differentiation efficiency. Our data provide novel insights and potential therapeutic targets for the clinical management of gestational diabetes mellitus.

Key words: high glucose; neural differentiation; autophagy; peroxisome proliferator-activated receptor gamma; P19 cells.

Introduction

Hyperglycemia induces serious complications and plays crucial role in the development of diabetic neuropathy, diabetic nephropathy, and diabetic retinopathy.[1,2] Diabetic neuropathy results from persistent exposure to high glucose (HG)-induced neuronal injury.[3-5] A recent report indicates that the global prevalence of diabetic neuropathy is approximately 30% in hospitalized diabetic patients and 20-30% in community-based diabetic patients.[6] Moreover, around 66% of type 1 and 59% of type 2 diabetic patients tend to develop diabetic neuropathy.[7,8] The expected global number of patients with diabetic neuropathy is predicted to double by 2030, reaching 20-30 million.[9] Diabetic neuropathy is a multifunctional disease with a complex pathogenesis involving the simultaneous involvement of multiple signaling pathways.[10-12] Gestational diabetes mellitus is initiated by elevated blood glucose levels in pregnant women and uncontrolled symptoms of this condition can elevate the risk of diabetic neuropathy in both the mother and the fetus.[13] Therefore, it is urgent to identify key molecular pathways of pathogenesis that can guide the development of drug targets for the prevention and treatment of neuropathy caused by gestational diabetes mellitus.

Autophagy, a cellular process for lysosomal degradation, plays a role in the recycling of longevity proteins, cytoplasm, and organelles.[14,15] This process is negatively regulated by the serine/threonine kinase mTOR (mammalian target of rapamycin) and is essential for cell growth and metabolism, as it helps maintain cellular homeostasis by degrading macromolecules.[16-18] The process starts with the formation of double-membrane autophagosomes, which sequester content and then fuse with acidic lysosomes to form autolysosomes, where the content is degraded by acid hydrolases to release the final product.[19] Over 30 autophagy-related protein (*Atg*) genes have been identified and classified to date, such as Atg8 and Atg12, which encode two ubiquitin-like proteins.[20] Atg12 binds to Atg5 *via* Atg7 and Atg10, E1 and E2-like proteins, while Atg7 and Atg3 bind Atg8/LC3-I to phosphatidylethanolamine (LC3-IPE/LC3-II).[21] Eventually, Atg12-Atg5 and Atg8 localize to develop autophagosomes and fuse with lysosomes upon completion.[22] The conversion of Beclin-1, LC3-I to LC3-II is an indicator of autophagosome formation and is widely used as a marker for inducing autophagy.[23] This pathway is largely dependent on lysosomal activity, and any defect in lysosomal degradation of autophagosomes can lead to their accumulation and impair cellular function, even resulting in cell death *via* protease activation.[24]

Neuronal differentiation is vital for fetal brain development, and autophagy critically affects neuronal differentiation from stem cells to neurons.[23,25] Embryonic stem cells are pluripotent stem cells that reside in early embryos with the ability to differentiate into the major germ layers: ectoderm, endoderm, and mesoderm.[26] Therefore, autophagy is critical for stem cell differentiation. Interestingly, some studies have observed impaired autophagosome formation in aberrant stem cell differentiation, suggesting that the autophagy pathway is inhibited and contributes to the reduction of cell volume and degradation of proteins.[27] Moreover, some key autophagy genes, such as homozygous mutations of Ambra1, lead to embryonic lethality in mice, and their deficiency in embryonic stem cells contributes to severe neural tube defects.[28] All of the above are associated with autophagy dysfunction and dysregulation.

Peroxisome proliferator-activated receptors (PPARs), a family of type II nuclear receptors, are ubiquitously expressed in tissues with cell type- and development stage-specific patterns.[29] Their transcriptional activity is regulated by steroid and lipid metabolites, and each member has a specific subset of genes responsible for lipid and energy metabolism.[30,31] PPAR activity is also regulated by post-translational modifications.[32] In the central nervous system (CNS), PPARs are expressed in all neural cell types and regulate many physiological processes, such as energy metabolism, redox homeostasis, autophagy, cell cycle, and differentiation.[33] After acute or chronic CNS injury, PPARs regulate various pathways, including neuroinflammation, antioxidant responses, and survival/neurodegenerative mechanisms.[34,35] PPARs have three isoforms (α, β/δ, and γ), and the γ isoform is the most studied among PPARs, especially PPARγ, which is tightly linked to autophagy.[36-42] A group reported that Agaricus bisporus-derived β-glucan prevents obesity through PPARγ downregulation and autophagy induction in zebrafish with yolk-fed.[43] In mice, the P38/PPAR-α pathway inhibits apoptosis and autophagy.[44] However, the role of PPARγ in neuronal differentiation *via* autophagy induction by HG remains poorly understood. To address this, we established a mouse stem cell model induced to differentiate into neuronal-like cells to investigate the impact of hyperglycemia on fetal nervous system development during pregnancy complicated by diabetes.

Materials and Methods

Cell culture

P19 cells were obtained from ATCC (https://www.atcc.org/products/crl-1825) and cultured according to ATCC guidelines. P19 cells are a commonly used embryonal carcinoma cell line derived from murine teratocarcinoma. These cells are capable of differentiating into various cell types, including neurons, muscle cells, and other types of cells, upon different treatment. In this model, treatment of P19 cells with RA leads to their differentiation into cells with characteristics of neurons, including the formation of neurites, expression of neuron-specific markers, and the ability to generate action potentials.[45] This approach has been used in a variety of studies to investigate various aspects of neuronal development, function, and disease.[46] The cells were maintained in Eagle's Minimum Essential Medium (#30-2003 from ATCC), supplemented with 2 mM L-Glutamine (Beyotime, Shanghai, China) and 10% (v/v) fetal bovine serum (FBS; Gibco, MA, USA) at 37°C with 5% CO_2.

Neural-like cells differentiation

P19 cells were seeded at a density of 2×10^4 cells/well onto a 6-well plate. Neural differentiation was initiated by the introduction of 0.5 μM all-trans retinoic acid (RA; Sigma-Aldrich, St. Louis, MO, USA), as previously described.[47] Additionally, cells were

Table 1. Primers used for RT-qPCR.

Primer	Primer sequence	Product size (bp)
gapdh	F: TGACCTCAACTACATGGTCTACA R: CTTCCCATTCTCGGCCTTG	85
map2	F: GCTGAGATCATCACACAGTC R: TCCTGCCAAGAGCTCATGCC	211
oct4	F: GGCGTTCTCTTTGGAAAGGTGTTC R: CTCGAACCACATCCTTCTCT	313
neun	F: GGCAAATGTTCGGGCAATTCG R: TCAATTTTCCGTCCCTCTACGAT	160
nanog	F: AAAGGATGAAGTGCAAGCGGTGG R: CTGGCTTTGCCCTGACTTTAAGC	520

maintained with a formulated medium containing Minimum Essential Medium (Sigma-Aldrich), 5% fetal bovine serum (Gibco), and 4 mM glutamine (Sigma-Aldrich) at 37°C with 5% CO_2. Differentiated cells were collected at day 1, 2, 3, and 4 for RT-PCR gene expression analysis, and cell morphology was observed by a phase-contrast microscope (IX81, Olympus, Hamburg, Germany).

High glucose treatment on neural-like cells

P19 cells were plated into 24-well plates at a density of 1×10^4 cells/well and cultured overnight. The cells were then treated with 30 mM glucose (HG group) or 5 mM glucose (normal glucose, NG group) during cell differentiation. Subsequently, the cells were treated with pharmacological compounds to modulate the activity of PPARγ, 100 nM Rosiglitazone (PPARγ agonist), or 10 μM T0070907 (PPARγ antagonist; both obtained from Cayman Chemicals (Ann Arbor, MI, USA), or transfected with shRNA plasmids or control. Differentiated cells were collected at day 3, 5, and 7 for further analysis.

RT-qPCR or RT-PCR

Total RNA was extracted using TRI-Reagent (Ambion, Invitrogen, Waltham, MA, USA) according to the manufacturer's instructions, as reported.[48] One microgram of total RNA was reverse transcribed using a cDNA kit (Applied Biosystems, Waltham, MA, USA) following the manufacturer's instructions. The resulting cDNA was used for amplification with primers specific for *gapdh*, *map2*, *oct4*, *neun*, and *nanog*, which are listed in Table 1. Nanog and Oct4 are stem cell markers, whereas NeuN and Map2 are neuron markers.[49] The data from three triplicate repeats were analyzed using the $2^{-\Delta\Delta Ct}$ method, and GAPDH was used as an internal control for normalization in each sample. PCR products were compared using gel electrophoresis.

Western blotting

This procedure was performed as in our previous report.[50] Protein extracts from cells were prepared in RIPA buffer (Beyotime) containing 1% NP-40 (Beyotime) and a cocktail of protease and phosphatase inhibitors (Beyotime). Protein concentrations were determined using the Bio-Rad protein assay (Bio-Rad, Hercules, CA, USA; 500-0006). Thirty micrograms of total protein were loaded onto 8-10% SDS-PAGE gels and transferred onto a PVDF membrane using a Trans-Blot Turbo SystemTM (Bio-Rad) and Transfer packTM (Bio-Rad; 1704156). The primary antibodies used for the analysis were as follows: Tuj1 (#ab18207; 1:1000; Abcam, Cambridge, UK), GFAP (ab7260; 1:1000; Abcam), LC3 (#ab128025; 1:500; Abcam), Beclin-1(#ab302669; 1:1000; Abcam), p62 (#ab207305;1:1000; Abcam), PPARγ (#ab178860; 1: 1000; Abcam), and GAPDH (1:1000; Beyotime). Protein bands were visualized using HRP-linked secondary antibodies (Bio-Rad, anti-mouse 1706516, anti-rabbit 1706515) and the Clarity Western ECL substrate (Bio-Rad, 1705061) with a ChemiDoc MP imaging system (Bio-Rad). The blots were stripped with glycine (0.2 M, pH 2.5) stripping buffer and reprobed with the appropriate antibodies. The intensity of each band was detected and measured by Image J software (version 1.4; National Institutes of Health, Bethesda, MD, USA; http://imagej.nih.gov/ij/).

Immunofluorescence

Cells were fixed with 4% PFA (#P0099; Beyotime) for at least 40 min at 4°C and incubated in blocking buffer containing 4% bovine serum albumin (BSA; Sigma-Aldrich) and 0.5% Triton X100
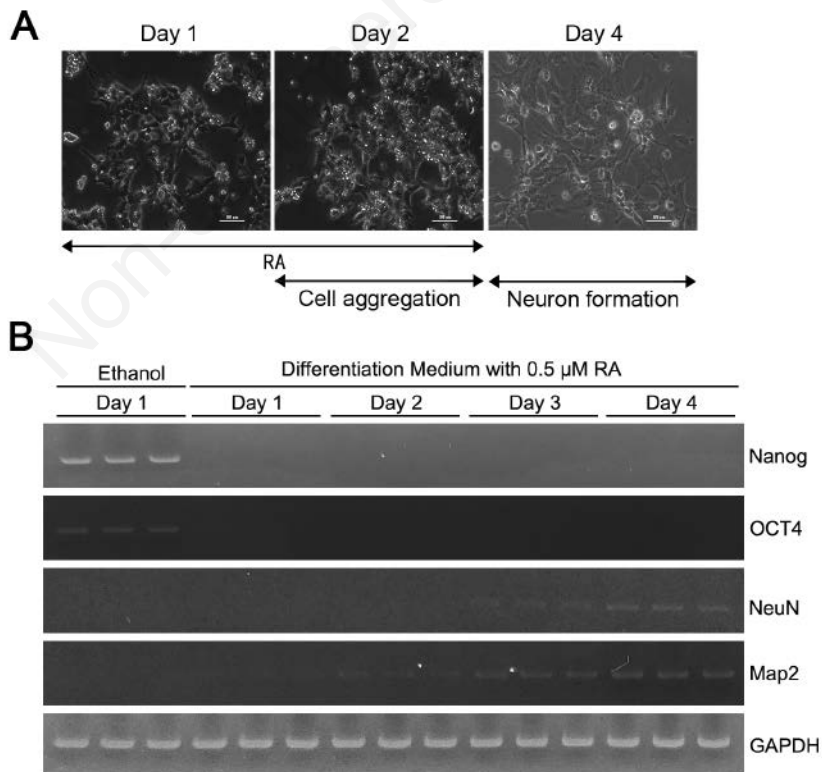
Figure 1. Effect of RA treatment on the transformation into neural-like cells in P19 cells. A) P19 cells were induced by 0.5 μM RA and the morphology in day 1, 2 and 4 were shown; scale bar: 10 μm. B) Products of Nanog, OCT4, NeuN and Map2 from RT-PCR were separated and shown in each day after induction of RA in P19 cells.

(Sigma-Aldrich) in PBS. The primary antibodies used for the analysis were the same as those used for the Western blotting assay. Primary antibodies were incubated overnight at 4°C. Cells were then washed with washing buffer (PBS, 0.1% Triton X100; Beyotime) and subsequently incubated with secondary antibodies conjugated with either Alexa Fluor 488 or 555 at 1:1000. Cells were washed three times with PBS and then stained with DAPI for nuclear staining (Bio-Rad). Confocal imaging was performed using a Leica TCS SP5 AOBS microscope system (Leica, Wetzlar, Germany), and image acquisitions were controlled using Leica LAS AF software (Leica). The positive staining rates of cells with Tuj1, GFAP or Map2 were calculated by merging with DAPI staining.

Flow cytometry

Flow cytometry was used to label apoptotic cells using an Annexin V-FITC kit (KeyGen Biotech, Nanjing, China), according to the manufacturer's instructions. Treated or untreated P19 cells were collected, washed twice in PBS, and resuspended at a concentration of 1×10^6 cells/mL. The cells were suspended in binding buffer and labeled with annexin V-FITC and propidium iodide for 10 min in the dark at 37°C. The cells were then analyzed using a FACS Calibur instrument and CellQuest Pro software version 3.3 (BD Biosciences, San Jose, CA, USA).

PPARγ silencing

For PPARγ silencing, siRNA oligos against PPARγ were designed and synthesized by GenePharm (Shanghai, China). The targeted sequences were as follows: shPPARγ-1#: 5'- GAGCT-GACCCAATGGTTGCTGATTA -3', 5'- shPPARγ-2#: CCAA-GAATACCAAAGTGCGATCAAA -3', and 5'- shPPARγ-3#: CCACTATGGAGTTCATGCTTGTGAA -3'. For transfection, the siRNA fragments or the negative control (NC) of 10 μL were loaded and transfected with Lipofectamine 2000 (Invitrogen) according to the manufacturer's instructions. After 24 h, the cells were incubated in induction media for 4 days.

Statistical analysis

Statistical analysis was performed using GraphPad Prism v5.0 (GraphPad Software, San Diego, CA, USA). Results from different experiments were analyzed, and all data were expressed as means ± SD. One-way ANOVA was used for statistical analysis of the data, followed by the Tukey *post-hoc* test for multiple group comparison and the Student's *t*-test for two-group comparison. A p-value less than 0.05 was considered statistically significant.

Results

The P19 cells differentiate successfully into neural-like cells upon retinoic acid treatment

After 1 day of 0.5 μM retinoic acid (RA) treatment, P19 cells began to aggregate, and a neural-like morphology was observed under a light microscope on day 4 (Figure 1A). Meanwhile, we evaluated the gene markers during neural stem cell differentiation to neural-like cells by RT-PCR. Compared with the vehicle control, differentiating P19 cells did not express Nanog and Oct4; however, the expression of NeuN and Map2 steadily increased from day 1 to day 4 (Figure 1B). Together, we successfully established the model of RA-induced P19 cell differentiation by identifying and characterizing cell phenotype and markers for later study.
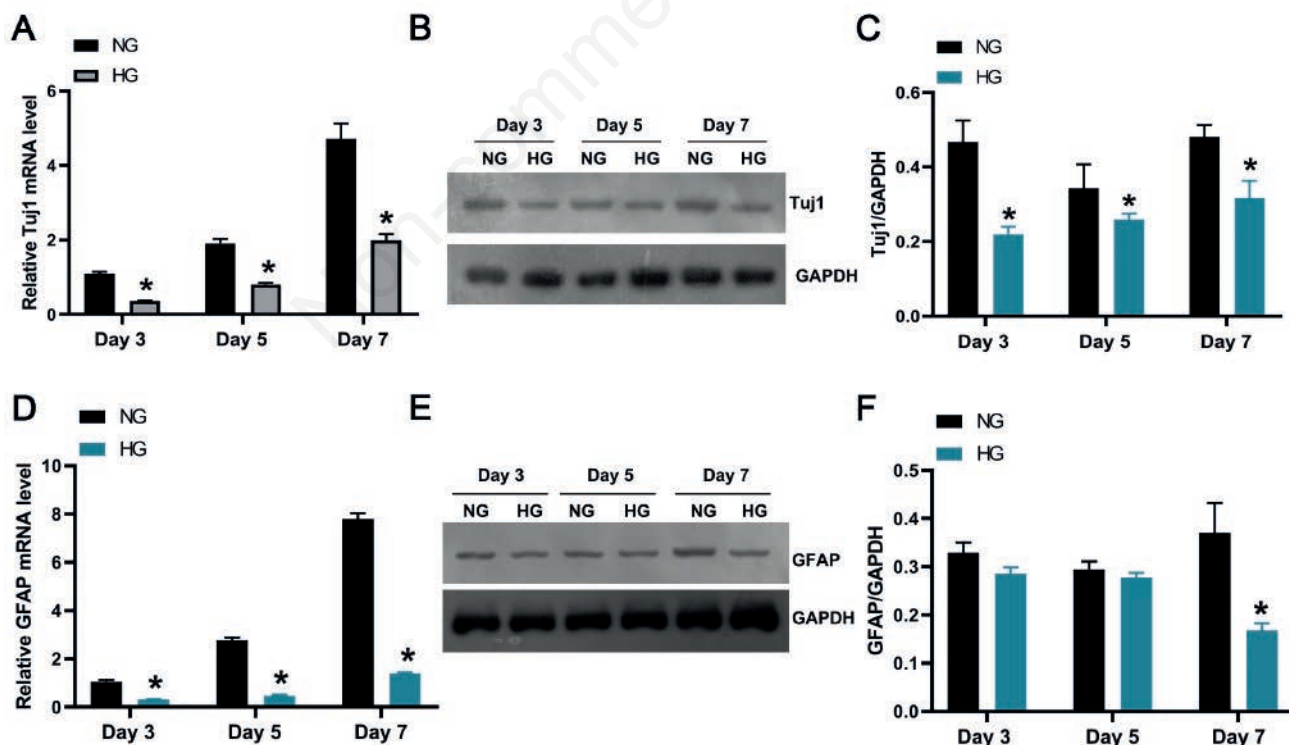
Figure 2. Effect of high glucose on the expression of Tuj1 and GFAP in P19 cells. A) P19 cells were treated with 30 mM glucose (HG group) or 5 mM glucose (normal glucose, NG group) and then subjected to RA induction. The mRNA (A) and protein (B,C) expression of Tuj1, or the mRNA (D) and protein (E,F) expression of GFAP were shown. *p<0.05.
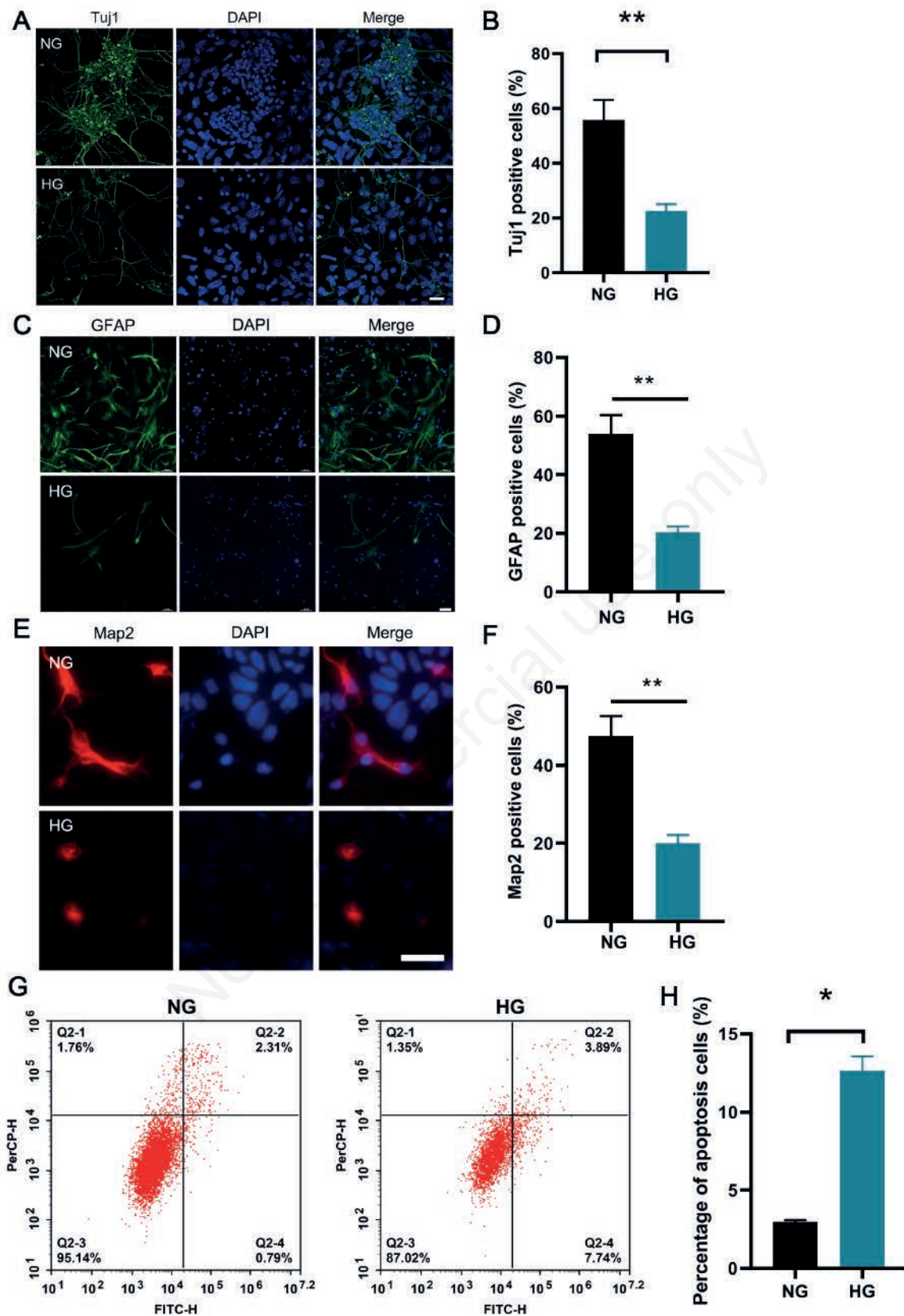
Figure 3. Effect of high glucose on the expression of Tuj1 and GFAP, and cell apoptosis in P19 cells. P19 cells were treated as in Figure 2 and subjected to immunocytochemistry for staining of Tuj1 (A,B), GFAP (C,D), and Map2 (E,F). Identical images of cells and the positive rate of induction were quantified. In addition, cells were subjected to flow cytometry to detect cell apoptosis (G), and the apoptosis rate was measured (H). Scale bars: 10 μm; *p<0.05; **p<0.01.

High glucose impedes the differentiation of P19 cells to neural-like cells, followed by an increase in cell apoptosis

According to literature reports, the proportion of P19 cell clusters induced into neurons generally ranges from 30% to 80%.[51-53] Here, in the current study, the percentage of RA-induced percentage of P19 transition into neuronal like cells was around 50%. To study the effect of HG on neural stem cell differentiation, we treated P19 cells during differentiation induction with a high level of glucose, with the purpose of simulating gestational hyperglycemia. After treatment with 30 mM glucose, we collected P19 cells and assessed the cell differentiation markers on day 3, day 5, and day 7. Tuj1, a neuron-specific marker, both in protein and mRNA, dramatically decreased from day 3 to day 7 (Figure 2 A-C). While GFAP, a glial marker, its mRNA significantly declined from day 3 to day 7, yet the protein only significantly decreased on day 7 (Figure 2 D-F). Furthermore, immunofluorescence staining showed that either Tuj1 (Figure 3 A,B) or GFAP (Figure 3 C,D) positive cells decreased by at least half. We also applied Map2 in immunofluorescence staining as a supplement. Map2 positive cells or immunofluorescence intensity significantly decreased (Figure 3 E,F), indicating that HG inhibits neural stem cell differentiation. To investigate the consequences of abnormal P19 cell differentiation, we analyzed cell apoptosis using flow cytometry. As shown in Figure 3 G,H, a significant increase in the number of apoptotic cells suggested that HG interrupted neural stem cell differentiation.

High glucose induces upregulation of autophagy during P19 cell differentiation

Furthermore, we confirmed that HG induces upregulation of autophagy during P19 cell differentiation by checking the expression of autophagy markers, p62, Beclin, and LC3 II/I, using Western blot analysis. Our results showed that levels of Beclin and LC3 II/I significantly increased, while p62 declined in P19 cells exposed to HG (Figure 4 A,B), indicating the upregulation of autophagy activity. As PPARγ is related to autophagy,[54] we evaluated its protein level using Western blot analysis (Figure 4). Both results showed that the expression of PPARγ increased significantly in the HG group compared to the normal glucose group, indicating that PPARγ may play an important role in HG-induced autophagy during neural stem cell differentiation.
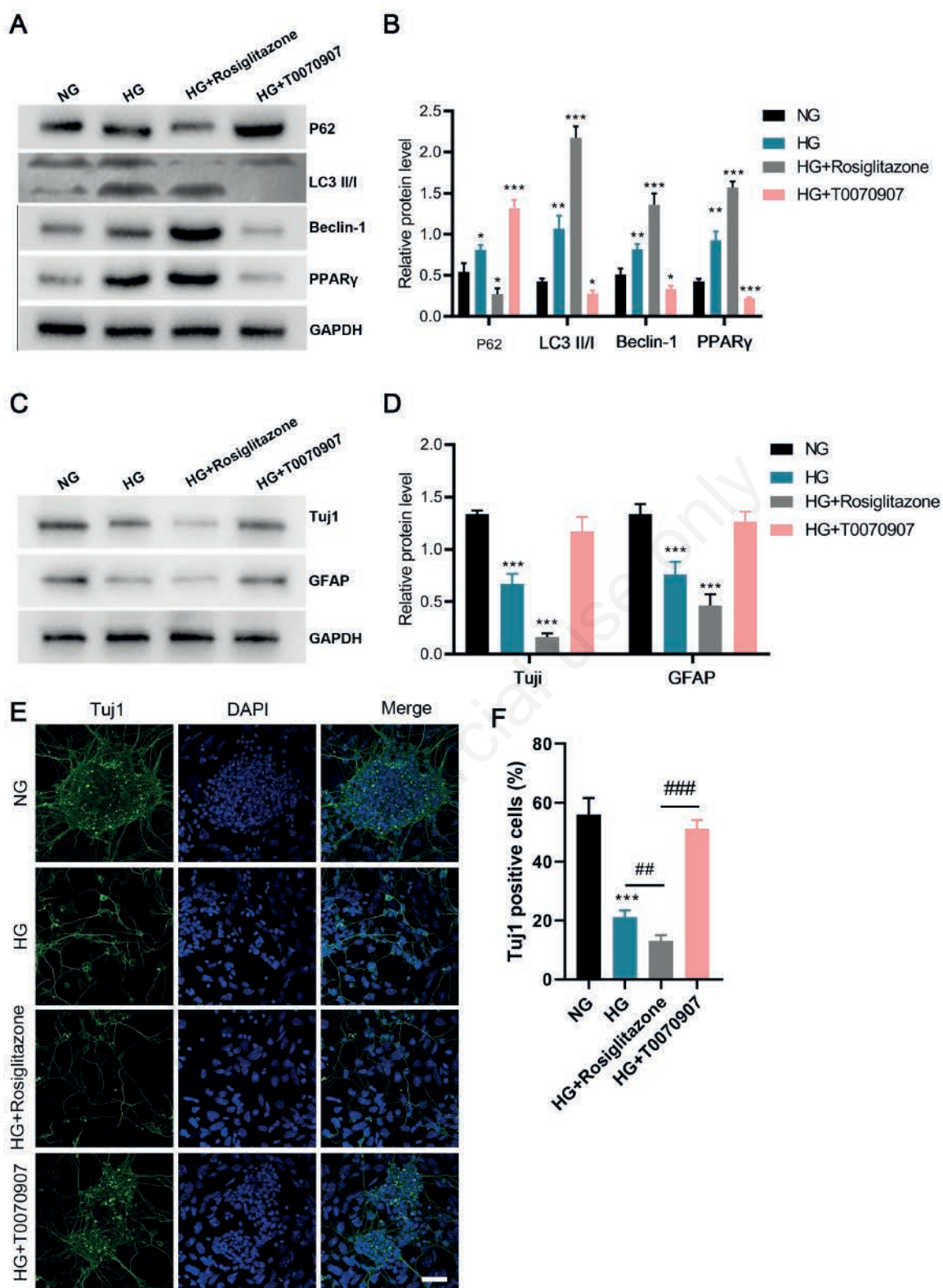
PPARγ is the regulator of excessive autophagy caused by high glucose during neuron differentiation

To further demonstrate the role of PPARγ on autophagy during differentiation induced by HG, we used pharmacological compounds, PPARγ agonist (Rosiglitazone) and antagonist (T0070907), to modulate PPARγ activity. The Western blot analysis showed that the protein levels of Beclin-1 and LC3 II/I dramatically increased, while p62 decreased in P19 cells treated with Rosiglitazone to promote PPARγ activity, implying more active autophagy (Figure 5 A,B). However, when we used T0070907 to reduce PPARγ activity, the decrease in Beclin and LC3 II/I and the increase in p62 suggested that autophagy was inhibited (Figure 5 A,B). Although PPARγ is known to be a key modulator of autophagy, its involvement in neuron differentiation is still unknown. Therefore, we tested the neural markers in P19 cells treated with either HG and Rosiglitazone or HG and T0070907. The western blot result showed a dramatic decrease in Tuj1 and GFAP in the Rosiglitazone-treated group compared to the solely HG-treated group (Figure 5 C,D). However, T0070907 rescued aberrant neural differentiation from the HG-treated group. These data suggest that the stimulation and blockage of PPARγ activity could either hinder or induce autophagy activity during neural differentiation with HG treatment, respectively. We also observed the same trend of Tuj1 and GFAP by immunofluorescence staining of P19 cells treated with either HG and Rosiglitazone or high glucose and T0070907, implying that PPARγ regulates autophagy during neural differentiation with HG treatment (Figure 5 E,F).

To further investigate the role of PPARγ in autophagy and neural differentiation, we applied gene manipulation to knockdown
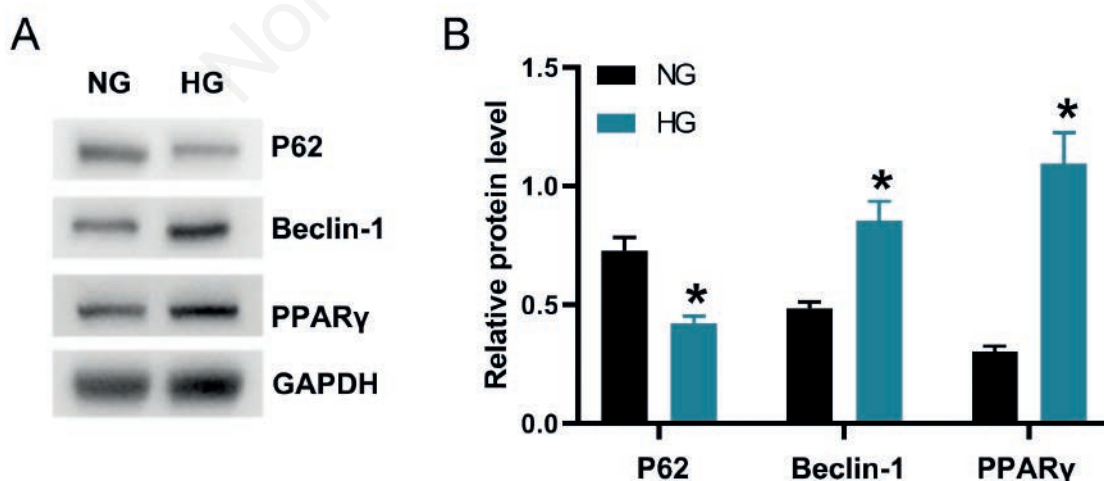

Figure 4. Effect of high glucose on autophagy during P19 cell differentiation. P19 cells were treated as in Figure 2 and cells were subjected to detect the expression level of P62, Beclin-1 and PPARγ, by Western blotting assay. The typical bands were shown in (A) and the relative expression levels were shown in (B).

Figure 5. PPARγ is the downstream regulator of excessive autophagy caused by high glucose during neuron differentiation. P19 cells were treated with HG, NG or PPARγ agonist (Rosiglitazone) and antagonist (T0070907) during RA induction. A) Cells were subjected to Western blotting assay to detect the levels of P62, Beclin-1, LC3 I/II, and PPARγ, and the quantified data were shown in (B). C,D) The expression levels of Tuj1 and GFAP were also detected and shown. E,F) Cells were subjected to immunocytochemistry for the detection of Tuj1, and the rate of Tuj1-positive cells was quantified. Scale bars: 10 μm; *p<0.05, **p<0.01, ***p<0.001, compared to NG group; ##p<0.01, ###p<0.001, compared to the HG group.
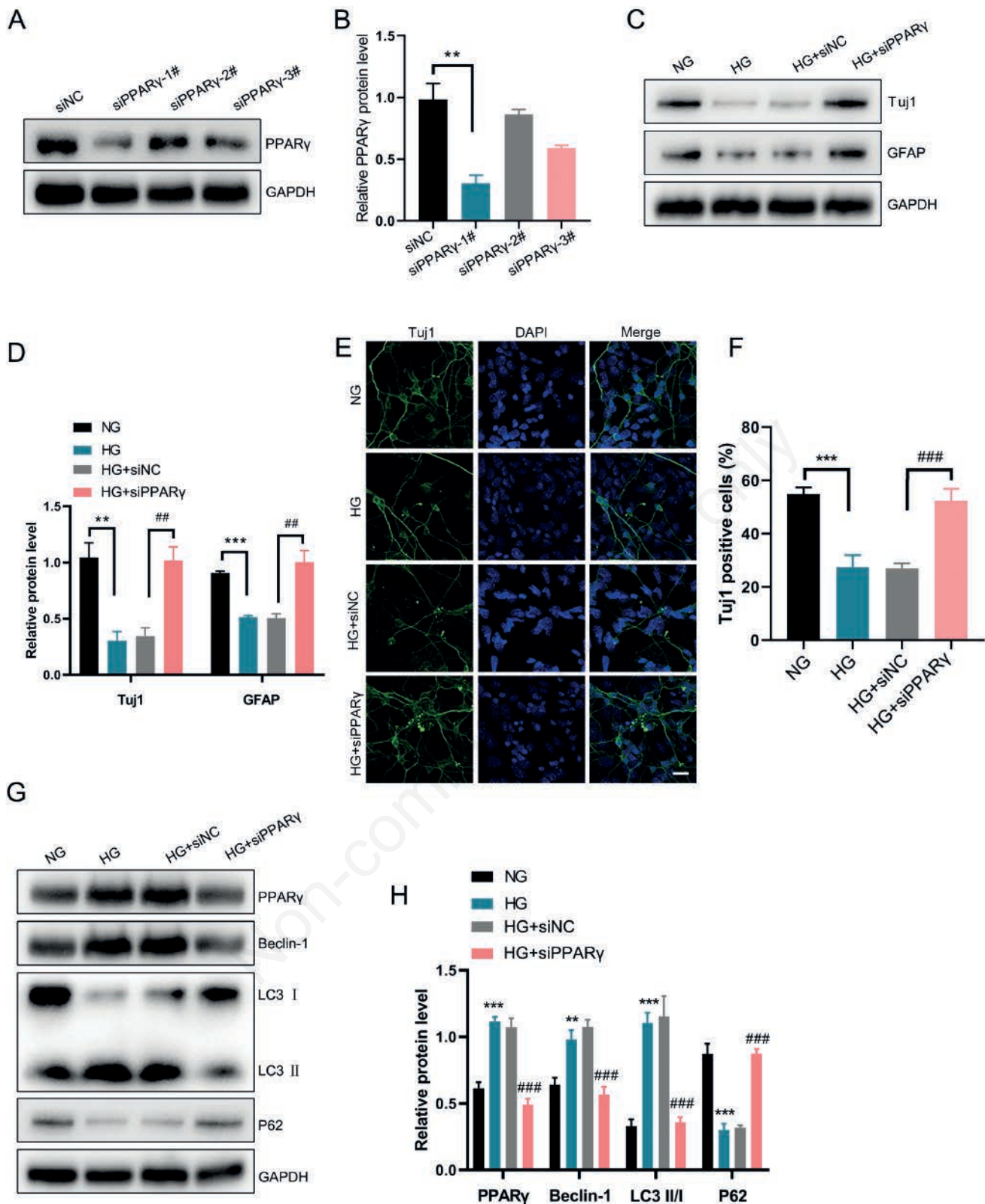
Figure 6. Genetic knockdown of PPARγ restores neuron differentiation impaired by HG treatment. P19 cells were treated with three indicated siRNA fragments against PPARγ, siNC (control), #1, #2 and #3 for 48 h. Then cells were collected for the detection of PPARγ by Western blotting (A,B). Then transfected cells were treated with NG, or HG and cells were subjected to Western blotting to detect Tuj1 and GFAP (C,D), or immunocytochemistry for Tuj1 staining (E,F), or P62, Beclin-1, LC3 I/II and PPARγ (G,H). Scale bars: 10 μm; *p<0.05, **p<0.01, ***p<0.001, compared to NG group; ##p<0.01, ###p<0.001, compared to HG+siNC group.

PPARγ. We designed three siRNA fragments against PPARγ and validated the knockdown efficiency by Western blot (Figure 6 A,B). We selected the most efficient siPPARγ (1#) for further experiments. We first monitored the autophagic activity in P19 cells after PPARγ knockdown, and the Western blot result showed that after PPARγ knockdown, the expression levels of both Tuj1 and GFAP in P19 cells significantly increased compared to the shNC group (Figure 6 C,D) as well as the result from immunofluorescence staining (Figure 6 E,F). Furthermore, the expression of Beclin-1 and LC3 II/I declined while that of p62 increased (Figure 6 G,H), indicating that the decrease of PPARγ inhibits autophagy activity. Notably, immunofluorescence staining showed a comparable increased number of Tuj1-positive P19 cells and decreased level of autophagic markers to the control group when they were treated with shPPARγ, suggesting that reduced PPARγ alleviates autophagy activity and rescues the deterioration of neural differentiation.

Discussion

In this study, we demonstrated that P19 cells maintained stemness by expressing stem cell markers (Oct4 and Nanog). Our first goal was to determine whether P19 cells could differentiate into neurons. After induction with RA, P19 cells exhibited a neural-like appearance and expressed neuron markers (Map2 and NeoN) in culture.

Among the complications of diabetes, clinical syndromes caused by damage to the peripheral and autonomic nervous systems are common.[55] These syndromes, generally referred to as different forms of neuropathy, are caused by diffuse and focal nervous system damage.[56] However, other types of diabetic neuropathy, such as pregestational maternal diabetes, cannot be ignored.[57] Persistently HG levels from pregestational maternal diabetes mellitus affect embryonic development by inducing structural defects, including neural tube defects (NTDs) and congenital heart defects.[55] Studies have demonstrated that interrupted neural differentiation from neural stem cells results in NTDs.[58] Maternal diabetes delays neural differentiation in the developing neuroepithelium, leading to NTD formation.[58,59] Therefore, we used this *in vitro* model, P19 cells, to investigate how HG influences embryonic stem cell differentiation into neural lineage cells. We used glucose at varying concentrations together with RA to study how glucose levels affect neural differentiation. After induction, we found that HG suppressed the induction of P19 cells into a neural phenotype, while an increasing subpopulation of P19 cells underwent apoptosis.

Prior studies have suggested that autophagy is involved in neural differentiation,[60] so we also monitored the activity of autophagy. We found increasing expression of LC3I/II and Beclin in cells treated with HG during neural differentiation. Hence, it could be hypothesized that autophagy plays a role in neuronal differentiation upon introduction of higher glucose. To further investigate the molecular mechanisms underlying this effect, we examined key molecules involved in orchestrating neuronal differentiation with excessive autophagy. Our findings suggest that HG levels can inhibit neural differentiation and induce apoptosis in P19 cells, potentially through the dysregulation of autophagic activity.

It is worth noting that PPARγ expression was significantly upregulated following HG treatment. PPARγ is a ligand-activated transcription factor of the nuclear hormone receptor superfamily, mainly present in the liver and lipid-rich organs, and plays a role in regulating metabolism.[61,62] PPARγ is activated to regulate autophagy, and PPARγ can also directly bind to DNA and regulate gene expression through transcription.[63] PPARγ can participate in a variety of physiological processes, including metabolism,

inflammation, cell growth and differentiation.[64] To investigate the role of PPARγ in regulating autophagy during neural differentiation, we utilized pharmacological agents to modulate its activity. Treatment with an antagonist resulted in decreased expression of both LC3I/II and Beclin in P19 cells, indicating that inhibiting PPARγ activity rescued neural differentiation under HG conditions. Conversely, treatment with an agonist further inhibited neural differentiation. Knockdown of PPARγ using molecular techniques produced similar results, further supporting the involvement of PPARγ-regulated autophagy in neuronal differentiation. While our findings suggest that HG levels impede P19 cell differentiation, it is important to note that glucose concentrations *in vivo* may not be equivalent to our experimental design. Additionally, blood glucose levels fluctuate throughout the day *in vivo*. Furthermore, our study only examined this phenomenon *in vitro*, and further investigation of PPARγ's effects in mouse models and eventually in patients is warranted.

In conclusion, our findings demonstrate that HG inhibits neural stem cell differentiation by upregulating autophagy activity through PPARγ, and the modulation of PPARγ activity can either hinder or induce autophagy activity during neural differentiation with HG treatment. Additionally, knockdown of PPARγ inhibits autophagy activity and rescues the deterioration of neural differentiation caused by HG treatment. These results shed light on the molecular mechanisms underlying the effects of HG on neural stem cell differentiation and suggest that PPARγ may serve as a potential target for the prevention and treatment of neurodegenerative diseases associated with HG levels.

References

1. Alexopoulos AS, Blair R, Peters AL. Management of preexisting diabetes in pregnancy: a review. JAMA 2019;321:1811-9.
2. Feghali MN, Umans JG, Catalano PM. Drugs to control diabetes during pregnancy. Clin Perinatol 2019;46:257-72.
3. Kapur A, McIntyre HD, Hod M. Type 2 diabetes in pregnancy. Endocrinol Metab Clin North Am 2019;48:511-31.
4. Ringholm L, Damm P, Mathiesen ER. Improving pregnancy outcomes in women with diabetes mellitus: modern management. Nat Rev Endocrinol 2019;15:406-16.
5. Etchegoyen M, Nobile MH, Baez F, Posesorski B, Gonzalez J, Lago N, et al. Metabolic syndrome and neuroprotection. Front Neurosci 2018;12:196.
6. Papanas N, Ziegler D. Risk factors and comorbidities in diabetic neuropathy: An update 2015. Rev Diabet Stud 2015; 12:48-62.
7. Oh J. Clinical spectrum and diagnosis of diabetic neuropathies. Korean J Intern Med 2020;35:1059-69.
8. Sasaki H, Kawamura N, Dyck PJ, Dyck PJB, Kihara M, Low PA. Spectrum of diabetic neuropathies. Diabetol Int 2020;11:87-96.
9. Caruso I, Marrano N, Biondi G, Genchi VA, D'Oria R, Sorice GP, et al. Glucagon in type 2 diabetes: Friend or foe? Diabetes Metab Res Rev 2023:e3609.
10. Malik RA. Diabetic neuropathy: A focus on small fibres. Diabetes Metab Res Rev 2020;36:e3255.
11. Feldman EL, Callaghan BC, Pop-Busui R, Zochodne DW, Wright DE, Bennett DL, et al. Diabetic neuropathy. Nat Rev Dis Primers 2019;5:41.
12. Zhang M, Zhou M, Cai X, Zhou Y, Jiang X, Luo Y, et al. VEGF promotes diabetic retinopathy by upregulating the PKC/ET/NF-kappaB/ICAM-1 signaling pathway. Eur J Histochem 2022;66:3522.
13. Bloomgarden ZT. Neuropathy, womens' health, and socioeco-

nomic aspects of diabetes. Diabetes Care 2002;25:1085-94.

14. Levine B, Kroemer G. Biological functions of autophagy genes: a disease perspective. Cell 2019;176:11-42.

15. Klionsky DJ, Emr SD. Autophagy as a regulated pathway of cellular degradation. Science 2000;290:1717-21.

16. Wullschleger S, Loewith R, Hall MN. TOR signaling in growth and metabolism. Cell 2006;124:471-84.

17. Lum JJ, DeBerardinis RJ, Thompson CB. Autophagy in metazoans: cell survival in the land of plenty. Nat Rev Mol Cell Biol 2005;6:439-48.

18. Noda T, Ohsumi Y. Tor, a phosphatidylinositol kinase homologue, controls autophagy in yeast. J Biol Chem 1998;273:3963-6.

19. Glick D, Barth S, Macleod KF. Autophagy: cellular and molecular mechanisms. J Pathol 2010;221:3-12.

20. Geng J, Klionsky DJ. The Atg8 and Atg12 ubiquitin-like conjugation systems in macroautophagy. 'Protein modifications: beyond the usual suspects' review series. EMBO Rep 2008;9:859-64.

21. Mizushima N, Komatsu M. Autophagy: renovation of cells and tissues. Cell 2011;147:728-41.

22. Johansen T, Lamark T. Selective autophagy: ATG8 family proteins, LIR motifs and cargo receptors. J Mol Biol 2020;432:80-103.

23. Stavoe AKH, Holzbaur ELF. Autophagy in neurons. Annu Rev Cell Dev Biol 2019;35:477-500.

24. Walls KC, Ghosh AP, Franklin AV, Klocke BJ, Ballestas M, Shacka JJ, et al. Lysosome dysfunction triggers Atg7-dependent neural apoptosis. J Biol Chem 2010;285:10497-507.

25. Benito-Cuesta I, Diez H, Ordonez L, Wandosell F. Assessment of autophagy in neurons and brain tissue. Cells 2017;6:25.

26. Mizushima N, Yamamoto A, Hatano M, Kobayashi Y, Kabeya Y, Suzuki K, et al. Dissection of autophagosome formation using Apg5-deficient mouse embryonic stem cells. J Cell Biol 2001;152:657-68.

27. Yue Z, Jin S, Yang C, Levine AJ, Heintz N. Beclin 1, an autophagy gene essential for early embryonic development, is a haploinsufficient tumor suppressor. Proc Natl Acad Sci USA 2003;100:15077-82.

28. Fimia GM, Stoykova A, Romagnoli A, Giunta L, Di Bartolomeo S, Nardacci R, et al. Ambra1 regulates autophagy and development of the nervous system. Nature 2007;447:1121-5.

29. Evans RM, Mangelsdorf DJ. Nuclear receptors, RXR, and the Big Bang. Cell 2014;157:255-66.

30. Braissant O, Foufelle F, Scotto C, Dauca M, Wahli W. Differential expression of peroxisome proliferator-activated receptors (PPARs): tissue distribution of PPAR-alpha, -beta, and -gamma in the adult rat. Endocrinology 1996;137:354-66.

31. Huin C, Corriveau L, Bianchi A, Keller JM, Collet P, Kremarik-Bouillaud P, et al. Differential expression of peroxisome proliferator-activated receptors (PPARs) in the developing human fetal digestive tract. J Histochem Cytochem 2000;48:603-11.

32. Barger PM, Browning AC, Garner AN, Kelly DP. p38 mitogen-activated protein kinase activates peroxisome proliferator-activated receptor alpha: a potential role in the cardiac metabolic stress response. J Biol Chem 2001;276:44495-501.

33. Moreno S, Farioli-Vecchioli S, Ceru MP. Immunolocalization of peroxisome proliferator-activated receptors and retinoid X receptors in the adult rat CNS. Neuroscience 2004;123:131-45.

34. Rolland B, Bordet R. The first theme issue on PPARs for brain disorders. Curr Drug Targets 2013;14:723.

35. Heneka MT, Landreth GE. PPARs in the brain. Biochim Biophys Acta 2007;1771:1031-45.

36. Kalinin S, Richardson JC, Feinstein DL. A PPARdelta agonist reduces amyloid burden and brain inflammation in a transgenic mouse model of Alzheimer's disease. Curr Alzheimer Res 2009;6:431-7.

37. Schnegg CI, Robbins ME. Neuroprotective mechanisms of PPARdelta: modulation of oxidative stress and inflammatory processes. PPAR Res 2011;2011:373560.

38. Heneka MT, Reyes-Irisarri E, Hull M, Kummer MP. Impact and therapeutic potential of PPARs in Alzheimer's disease. Curr Neuropharmacol 2011;9:643-50.

39. Barroso E, del Valle J, Porquet D, Vieira Santos AM, Salvado L, Rodriguez-Rodriguez R, et al. Tau hyperphosphorylation and increased BACE1 and RAGE levels in the cortex of PPARbeta/delta-null mice. Biochim Biophys Acta 2013;1832:1241-8.

40. Benedetti E, D'Angelo B, Cristiano L, Di Giacomo E, Fanelli F, Moreno S, et al. Involvement of peroxisome proliferator-activated receptor beta/delta (PPAR beta/delta) in BDNF signaling during aging and in Alzheimer disease: possible role of 4-hydroxynonenal (4-HNE). Cell Cycle 2014;13:1335-44.

41. Corbett GT, Gonzalez FJ, Pahan K. Activation of peroxisome proliferator-activated receptor alpha stimulates ADAM10-mediated proteolysis of APP. Proc Natl Acad Sci USA 2015;112:8445-50.

42. Skerrett R, Pellegrino MP, Casali BT, Taraboanta L, Landreth GE. Combined liver X receptor/peroxisome proliferator-activated receptor gamma agonist treatment reduces amyloid beta levels and improves behavior in amyloid precursor protein/presenilin 1 mice. J Biol Chem 2015;290:21591-602.

43. Li X, Xue Y, Pang L, Len B, Lin Z, Huang J, et al. Agaricus bisporus-derived beta-glucan prevents obesity through PPAR gamma downregulation and autophagy induction in zebrafish fed by chicken egg yolk. Int J Biol Macromol 2019;125:820-8.

44. Lu X, Liu T, Chen K, Xia Y, Dai W, Xu S, et al. Isorhamnetin: A hepatoprotective flavonoid inhibits apoptosis and autophagy via P38/PPAR-alpha pathway in mice. Biomed Pharmacother 2018;103:800-11.

45. Gonzalez-Blanco L, Bermejo-Millo JC, Oliveira G, Potes Y, Antuna E, Menendez-Valle I, et al. Neurogenic potential of the 18-kDa mitochondrial translocator protein (TSPO) in pluripotent P19 stem cells. Cells 2021;10:2784.

46. Prasad R, Jung H, Tan A, Song Y, Moon S, Shaker MR, et al. Hypermethylation of Mest promoter causes aberrant Wnt signaling in patients with Alzheimer's disease. Sci Rep 2021;11:20075.

47. Rudnicki MA, Ruben M, McBurney MW. Regulated expression of a transfected human cardiac actin gene during differentiation of multipotential murine embryonal carcinoma cells. Mol Cell Biol 1988;8:406-17.

48. Berardo C, Siciliano V, Di Pasqua LG, Richelmi P, Vairetti M, Ferrigno A. Comparison between lipofectamine RNAiMAX and GenMute transfection agents in two cellular models of human hepatoma. Eur J Histochem 2019;63:3048.

49. Anji A, Anderson B, Akhtar F, Meekins DA, Ito T, Mummidi S, et al. Exosomes induce neurogenesis of pluripotent P19 cells. Stem Cell Rev Rep 2023. Online Ahead of Print.

50. Liu H, Cai X, Liu J, Zhang F, He A, Li R. The MEG3 lncRNA promotes trophoblastic cell growth and invasiveness in preeclampsia by acting as a sponge for miR-21, which regulates BMPR2 levels. Eur J Histochem 2021;65:3323.

51. Voronova A, Fischer A, Ryan T, Al Madhoun A, Skerjanc IS. Ascl1/Mash1 is a novel target of Gli2 during Gli2-induced neurogenesis in P19 EC cells. PLoS One 2011;6:e19174.

52. Fu F, Li LS, Li R, Deng Q, Yu QX, Yang X, et al. All-trans-retinoid acid induces the differentiation of P19 cells into neu-

OPEN ACCESS

rons involved in the PI3K/Akt/GSK3beta signaling pathway. J Cell Biochem 2020;121:4386-96.

53. Moazeny M, Dehbashi M, Hojati Z, Esmaeili F. Investigating neural differentiation of mouse P19 embryonic stem cells in a time-dependent manner by bioinformatic, microscopic and transcriptional analyses. Mol Biol Rep 2022;50:2183-94.

54. Faghfouri AH, Khajebishak Y, Payahoo L, Faghfuri E, Alivand M. PPAR-gamma agonists: Potential modulators of autophagy in obesity. Eur J Pharmacol 2021;912:174562.

55. Ziegler D, Keller J, Maier C, Pannek J. Diabetic neuropathy. Exp Clin Endocrinol Diabetes 2023;131:72-83.

56. Hackett RA, Steptoe A. Type 2 diabetes mellitus and psychological stress - a modifiable risk factor. Nat Rev Endocrinol 2017;13:547-60.

57. Gabbay-Benziv R, Reece EA, Wang F, Yang P. Birth defects in pregestational diabetes: Defect range, glycemic threshold and pathogenesis. World J Diabetes 2015;6:481-8.

58. Lee SY, Papanna R, Farmer D, Tsao K. Fetal repair of neural tube defects. Clin Perinatol 2022;49:835-48.

59. Ocal O, Ocal FD, Sinaci S, Daglar Z, Secen AE, Divanlioglu D, et al. Maternal serum and fetal cord blood concentrations of thiol/disulfide and ischemia-modified albumin as predictors of neural tube defects. Turk Neurosurg 2023;33:134-9.

60. Hong CJ, Park H, Yu SW. Autophagy for the quality control of adult hippocampal neural stem cells. Brain Res 2016;1649:166-72.

61. Qi Y, Zhang M, Li H, Frank JA, Dai L, Liu H, et al. Autophagy inhibition by sustained overproduction of IL6 contributes to arsenic carcinogenesis. Cancer Res 2014;74:3740-52.

62. Strand DW, Jiang M, Murphy TA, Yi Y, Konvinse KC, Franco OE, et al. PPARgamma isoforms differentially regulate metabolic networks to mediate mouse prostatic epithelial differentiation. Cell Death Dis 2012;3:e361.

63. Corona JC, de Souza SC, Duchen MR. PPARgamma activation rescues mitochondrial function from inhibition of complex I and loss of PINK1. Exp Neurol 2014;253:16-27.

64. Liu Y, Wang J, Luo S, Zhan Y, Lu Q. The roles of PPARgamma and its agonists in autoimmune diseases: A comprehensive review. J Autoimmun 2020;113:102510.